

Decrease in Tumor Cell Oxygen Consumption after Treatment with Vandetanib (ZACTIMA™; ZD6474) and its Effect on Response to Radiotherapy

Réginald Ansiaux,^a Julie Dewever,^b Vincent Grégoire,^c Olivier Feron,^b Bénédicte F. Jordan^a and Bernard Gallez^{a,b,1}

^a Biomedical Magnetic Resonance Unit, Louvain Drug Research Institute, Université Catholique de Louvain, B-1200 Brussels, Belgium;

^b Laboratory of Pharmacology and Therapeutics, Université Catholique de Louvain, B-1200 Brussels, Belgium; and ^c Laboratory of Molecular Imaging and Experimental Radiotherapy, Université Catholique de Louvain, B-1200 Brussels, Belgium

Ansiaux, R., Dewever, J., Grégoire, V., Feron, O., Jordan, B. F. and Gallez, B. Decrease in Tumor Cell Oxygen Consumption after Treatment with Vandetanib (ZACTIMA™; ZD6474) and its Effect on Response to Radiotherapy. *Radiat. Res.* 172, 584–591 (2009).

We investigated the early effects of vandetanib (ZACTIMA™; ZD6474), an inhibitor of VEGFR-dependent angiogenesis, on tumor oxygenation and on the possible consequences of combining vandetanib with radiotherapy. Tumor oxygenation, perfusion, cellular consumption of oxygen, and radiation sensitivity were studied in transplantable liver tumors after daily doses of vandetanib (25 mg kg⁻¹ i.p.). Measurements of oxygenation (pO₂) and tumor cell oxygen consumption were carried out using electron paramagnetic resonance (EPR), and perfusion parameters were assessed by dynamic contrast-enhanced magnetic resonance imaging (DCE-MRI). Regrowth delay assays were performed after treatment with vandetanib alone, radiation alone or a combination of both treatments. Vandetanib induced an early increase in tumor oxygenation that did not correlate with remodeling of the tumor vasculature or with changes in tumor perfusion. A decrease in tumor cell oxygen consumption was observed that could have been responsible for this increase in tumor oxygenation. Consistent with this increase in tumor oxygenation, we found that vandetanib potentiated the tumor response to radiotherapy. Our results confirm that treatment with an inhibitor of VEGFR signaling reduces oxygen consumption rate by tumor cells. The observation that vandetanib causes an early increase in tumor oxygenation has implications for the timing and sequencing of treatment with VEGF signaling inhibitors in combination with radiation. © 2009 by Radiation Research Society

INTRODUCTION

The widely accepted mechanism of action of anti-angiogenic drugs as cancer therapy alone or in combination with other treatments is that they prevent the

formation of new tumor blood vessels, thus inhibiting tumor cell growth (1). In addition to this long-term “starvation” effect, the emerging concept of a transient tumor vascular “normalization” during the early phase of anti-angiogenic treatment (2) has recently been confirmed by various preclinical (3–12) and clinical studies (13, 14). This concept suggests that anti-angiogenic agents first prune the immature and inefficient blood vessels and then induce a remodeling of the remaining vasculature, leading to a transiently improved tumor perfusion (2, 15). Benefits can be taken from this more efficient delivery of oxygen and nutrients to tumor cells by combining anti-angiogenic agents with radiation and chemotherapy during this normalization period (3, 4). However, the evolution of the tumor microenvironment during anti-angiogenic treatment is complex, and the normalization process does not appear to be the only change occurring during the early phase. We recently reported that SU5416, a selective inhibitor of VEGFR-2 (Flk-1/KDR), induced early tumor reoxygenation by a mechanism that was not associated with an effect on tumor perfusion but rather was linked to an inhibition of mitochondrial respiration (16). Consistent with these findings, a significant benefit was observed when SU5416 was associated with radiotherapy but not with chemotherapy. This was likely the consequence of tumor reoxygenation without improvement in the perfusion. A key question is whether this mechanism of reoxygenation (inhibition of oxygen consumption or transient normalization) is common to other anti-angiogenic agents that target VEGFR-2.

In the present study, we used vandetanib, a low-molecular-weight inhibitor of VEGFR-2 tyrosine kinase with additional activity against EGFR (epidermal growth factor receptor) and RET (relocated during transfection) tyrosine kinases (17, 18). Initial preclinical studies with vandetanib have shown antitumor activity in a variety of human tumor xenografts that is consistent with an anti-angiogenic effect (17–19). In addition, vandetanib may have a direct inhibitory effect on tumor cell growth and

¹ Address for correspondence: Biomedical Magnetic Resonance unit, Université catholique de Louvain, Avenue E. Mounier 73.40, B-1200 Brussels, Belgium; e-mail: bernard.gallez@uclouvain.be.

survival in tumors that are dependent on EGFR and/or RET signaling.

To characterize the changes in the tumor microenvironment induced by vandetanib, we used multiple modalities. Contrast-enhanced magnetic resonance imaging (MRI) has been used to measure tumor perfusion non-invasively (23), electron paramagnetic resonance (EPR) oximetry has been used to monitor pO_2 *in vivo* repeatedly and relatively non-invasively (24, 25), and oxygen consumption has been measured *ex vivo* using EPR. The transplantable liver tumor (TLT) model was used because the effects of other anti-angiogenic agents (thalidomide, SU5416) have already been characterized in this model (4, 16). The aim of the current study was to offer a rationale for combining vandetanib with radiotherapy and to dissect the underlying mechanisms responsible for radiosensitization.

MATERIAL AND METHODS

Mice and Tumor Models

Approximately 10^6 murine TLT cells (26) in 0.1 ml of medium were injected i.m. into the right thighs of male NMRI mice. Mice developed palpable tumors within a week of inoculation. Tumor size was measured daily with an electronic caliper. Animals were anesthetized by inhalation of isoflurane mixed with 21% oxygen (air) in a continuous flow (1.5 liter/h), delivered by a nose cone (3% for induction, 1.5% for maintenance). To maintain normothermia, mice were placed on a heating pad (37°C) for all experiments except for the DCE-MRI experiment, where warm air was flushed into the magnet. All animal experiments were conducted in accordance with national animal care regulations.

Treatments

Vandetanib was provided by AstraZeneca (Macclesfield, UK). For the treated group, vandetanib was dissolved in dimethyl sulfoxide (DMSO, Sigma Aldrich, Bornem, Belgium) and was administered intraperitoneally (i.p.) at a dose of 25 mg/kg body weight once a day via a 100- μ l injection. Control animals were treated with DMSO only. Treatment with vandetanib was started when tumors reached a diameter of 7.5 ± 0.5 mm, approximately 7 days after tumor inoculation. The treatment protocol is detailed in Fig. 1.

Tumor Oxygenation

Electronic paramagnetic resonance (EPR) oximetry, using charcoal (CX0670-1, EM Science, Gibbstown, NJ) as the oxygen-sensitive probe was used to evaluate changes in tumor oxygenation after treatment with vandetanib using a protocol described previously (24). The technique is intended for continuous measurement of local pO_2 without altering the local oxygen concentration. Briefly, EPR spectra were recorded using an EPR spectrometer (Magnetech, Berlin, Germany) with a low-frequency microwave bridge operating at 1.2 GHz and an extended loop resonator. A suspension of charcoal was injected via a 26G needle in the center of the tumor 1 day before measurement (100 mg/ml, 50 μ l injected, 1–25- μ m particle size). Acquisition parameters were the following: 1-min scans, field sweep: 1.0 mT, amplitude modulation: less than one-third of the line width, two averages, 100 kHz. Calibration curves were made by measuring the EPR line width as a function of the pO_2 . For this purpose, the charcoal was suspended in a tumor homogenate, and EPR spectra were obtained on a Bruker EMX EPR spectrometer (9 GHz) between 0 and 21% O_2 .

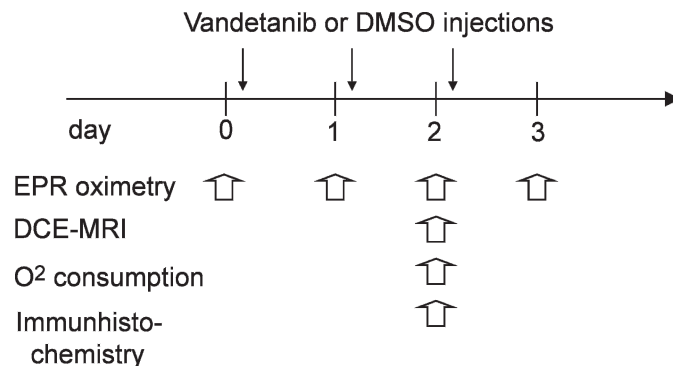


FIG. 1. Schematic representation of the treatment protocol for each technique.

Nitrogen and air were mixed in an Aalborg gas mixer (Monsey, NY), and the oxygen content was analyzed using a Servomex oxygen analyzer OA540 (Analytic Systems, Brussels, Belgium). The localized EPR measurements correspond to an average of pO_2 values in a volume of ~ 10 mm³ (24). To avoid any acute effect of the treatment, data were acquired before the injection of vandetanib ($n = 8$) or DMSO ($n = 5$) and then on a daily basis from day 0 until day 3 (daily EPR measurement followed by injection of treatment or vehicle).

Flow Measurements

Dynamic contrast enhanced magnetic resonance imaging (DCE MRI) was used to assess changes in tumor perfusion and permeability 24 h after the second vandetanib ($n = 6$) or DMSO injection ($n = 5$) (corresponding to day 2 in Fig. 1, i.e., the time of maximal increase in pO_2). Single-slice DCE-MRI was done with a 4.7 T (200 MHz, ¹H) 40-cm-inner-diameter bore system (Bruker Biospec, Ettlingen, Germany) using the rapid-clearance blood pool agent P792 (Vistarem®, Guerbet, Roissy, France) (27). High-resolution multi-slice T₂-weighted spin echo anatomic imaging was performed just before dynamic contrast-enhanced imaging. Pixel-by-pixel values for K^{trans} (influx volume transfer constant, from plasma into the interstitial space, units of min⁻¹), V_p (blood plasma volume per unit volume of tissue, unitless), and K_{ep} (fractional rate of efflux from the interstitial space back to blood, units of min⁻¹) in the tumor were calculated by tracer kinetic modeling of the dynamic contrast-enhanced data (27), and the resulting parametric maps for K^{trans} , V_p and K_{ep} were generated. Statistical significance for V_p or K^{trans} identified “perfused” pixels (i.e., pixels to which the contrast agent P792 had access) (27, 28).

Evaluation of Oxygen Consumption Rate

The method described by Jordan *et al.* (29) was used. All spectra were recorded on a Bruker EMX EPR spectrometer operating at 9 GHz. TLT tumor-bearing mice were treated for 2 days with vandetanib ($n = 4$) at a dose of 25 mg/kg via 100- μ l i.p. injection or with DMSO ($n = 3$). Twenty-four hours after the second injection, the mice were killed humanely and the tumor was excised. TLT tumors were then dissected in a sterile environment and gently pieced in McCoy’s medium. The cell suspension was trypsinized, filtered (100- μ m size pore nylon filter, Millipore, Brussels, Belgium) and centrifuged (5 min, 1500g/min, 4°C) before cell viability was determined. Cells were suspended in 10% dextran in complete medium A neutral nitroxide, ¹⁵N 4-oxo-2,2,6,6-tetramethylpiperidine-d₁₆-¹⁵N-1-oxyl at 0.2 mM (CDN Isotopes, Pointe-Claire, Quebec, Canada), was added to 100- μ l aliquots of tumor cells that were then drawn into glass capillary tubes. The sealed tubes were placed into quartz EPR tubes, and samples were maintained at 37°C. Because the resulting line width reports on O_2 concentration, oxygen consumption rates were obtained by measuring the O_2 concentration

in the closed tube over time and finding the slope of the resulting linear plot. The probe (0.2 mM in 20% dextran in complete medium) was calibrated at various O₂ concentrations between 100% nitrogen and air so that the line-width measurements could be related to any value of O₂ concentration. Nitrogen and air were mixed in an Aalborg gas mixer, and the oxygen concentration was analyzed using a Servomex OA540 oxygen analyzer.

Radiation Sensitivity In Vivo

The TLT tumor-bearing leg was irradiated locally with 10 Gy of 250 kV X rays (RT 250; Philips Medical Systems). The tumor was centered in a 3-cm-diameter circular irradiation field. A single-dose irradiation of 10 Gy was given 24 h after the second injection of vandetanib. After radiotherapy, tumor growth was determined daily by measuring transverse and antero-posterior tumor diameters until they reached 16 mm, at which time the mice were killed. A linear fit was performed between 8 and 16 mm that allowed determination of the time to reach a particular size (12-mm tumor diameter) for each mouse.

Radiation Sensitivity In Vitro

TLT tumors in mice were dissected in a sterile environment and gently pieced in McCoy's medium. The cell suspension was filtered (100- μ m size pore nylon filter, Millipore, Brussels, Belgium) and centrifuged (5 min, 450g, 4°C), and cells were cultured in DMEM containing 10% fetal bovine serum. Confluent cells were treated with vandetanib (5 μ M) 2 h before being irradiated at 2 Gy. To assess cell radiosensitivity, the Trypan blue exclusion dye assay was performed; cells were counted for viability 24 h after irradiation. The experiments were carried out in triplicate. It should be noted that it was impossible to use the classical clonogenic assay with this model because colonies do not form.

Immunohistochemistry

TLT tumor-bearing mice were killed after 2 days of treatment with vandetanib ($n = 5$) or DMSO ($n = 4$). Tumor cryoslices were immunoprobed with rat monoclonal CD31 IgG2a antibodies (PharMingen, San Diego, CA). Rabbit polyclonal anti-rat IgG peroxidase-conjugated antibodies (Jackson ImmunoResearch Laboratories, West Grove, PA) and AEC (amino ethyl carbazol) substrate system (DakoCytomation, Heverlee, Belgium) were used for revelation; sections were then counterstained with Mayer's hematoxylin. Quantification of the peroxidase signal was performed using dedicated Axiovision 4.6.3 software (Carl Zeiss, Germany) on representative images captured with a CCD camera.

Statistical Analysis

Results are given as means \pm SEM from n animals. Comparisons between groups were made with Student's two-tailed t test or two-way ANOVA where appropriate, and a P value less than 0.05 was considered significant.

RESULTS

Effect of Vandetanib on Tumor Oxygenation

EPR oximetry is designed for continuous measurement of the local pO₂ without altering the local oxygen concentration; it allows repeated, real-time measurements from the same tissue over long periods (24). The initial TLT pO₂ was measured on day 0 (before any treatment) and was similar in both groups (vandetanib, 2.3 \pm 0.3 mmHg, $n = 8$; control group, 2.5 \pm 0.3 mmHg, $n = 5$). Daily vandetanib injections significantly modified

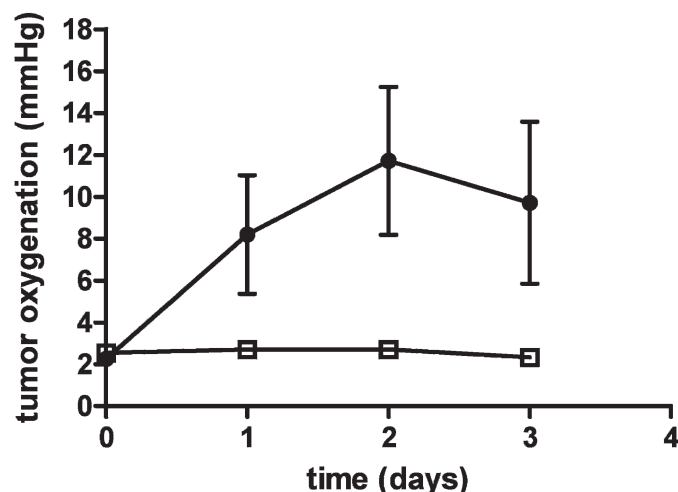


FIG. 2. Effect of daily vandetanib injection on TLT tumor oxygenation monitored by EPR oximetry. \square , Control group ($n = 5$); \blacksquare , treated group ($n = 8$). Note the significant increase in pO₂ 24 h after the first injection, with a maximum on day 2. Points, means; bars, SE; **, $P < 0.01$.

tumor pO₂ (Fig. 2). For the treated group, tumor oxygenation increased after the first administration of vandetanib and reached a maximum after 2 days (11.7 \pm 3.5 mmHg), followed by a continuous decrease in pO₂. No such pO₂ increase was observed for the control group. Tumor pO₂ was significantly different between vandetanib-treated tumors and controls (two-way ANOVA). All further experiments for the tumor characterization and determination of the therapeutic relevance of treatment with vandetanib were conducted on day 2 (as illustrated Fig. 1), the time of maximal reoxygenation.

Effects of Vandetanib on Tumor Perfusion

Tumor perfusion was monitored in the TLT tumors 24 h after the second injection of vandetanib by dynamic contrast-enhanced MRI at 4.7 T using i.v. injection of the rapid-clearance blood pool agent P792 (Vistarem[®]) (27). The pixel-by-pixel analysis generated "perfusion maps" (using the values for V_p, the blood plasma volume per unit volume of tissue) and "permeability maps" (using the values for K^{trans}, the influx volume transfer constant, from plasma into the interstitial space, and K_{ep}, the efflux volume transfer constant from the interstitial space back to plasma). Moreover, the kinetic analysis identified "perfused pixels" (i.e., pixels to which the contrast agent had access, showing a statistical significance for V_p or K^{trans}) (27). The fraction of perfused pixels for the tumors treated with vandetanib (Fig. 3A) was not significantly different than that of controls (64.6 \pm 4.3%, $n = 6$, compared to 70.8 \pm 3.9% $n = 5$, respectively, $P > 0.05$, Student's t test). No differences in the average values of K^{trans}, K_{ep} or V_p were observed between tumors treated with vandetanib or DMSO (Fig. 3B, C). These results indicate that vandetanib did not change tumor perfusion parameters at this time of treatment in this tumor model.

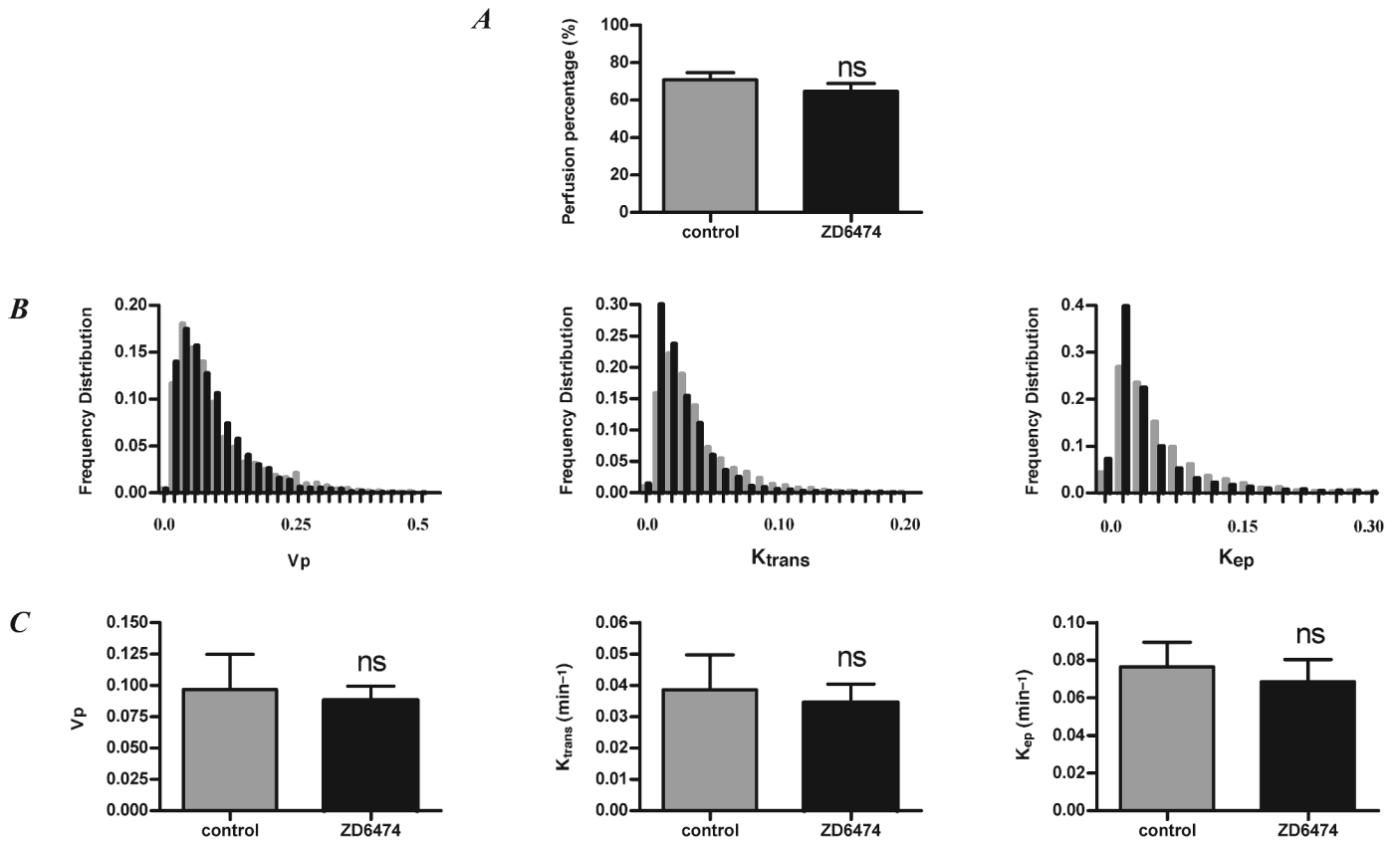


FIG. 3. Tumor perfusion and permeability as measured by DCE-MRI. Panel A: Mean percentage of perfused pixels in the treated ($n = 6$) and control groups ($n = 5$). Panel B: Distribution of vascular parameters in tumors treated with DMSO or vandetanib. V_p is the blood plasma volume per unit volume of tissue, K_{trans} is the influx volume transfer constant from plasma into the interstitial space, and K_{ep} is the efflux volume transfer constant from the interstitial space back to the plasma. Panel C: Overall estimation of pharmacokinetic parameters after vandetanib treatment. Columns, means; bars, SE; ns, not significant.

Histological Analysis

Immunohistological staining with an antibody directed against CD31 was used to investigate whether tumor vascularization and organization were modified 2 days after vandetanib treatment (Fig. 4). The examination of histological sections by independent observers indicated that tumor vessels were distributed uniformly throughout

the tumors in both the control and treated groups. No apparent decrease in the number of vessels was observed after vandetanib treatment, and the overall vessel diameter distribution was similar in control and treated animals, contrary to observations made after treatment with thalidomide (3). The quantification of fluorescence showed no significant difference between groups [$100.0 \pm 6.0\%$ compared to $92.7 \pm 7\%$ for control ($n = 4$) and

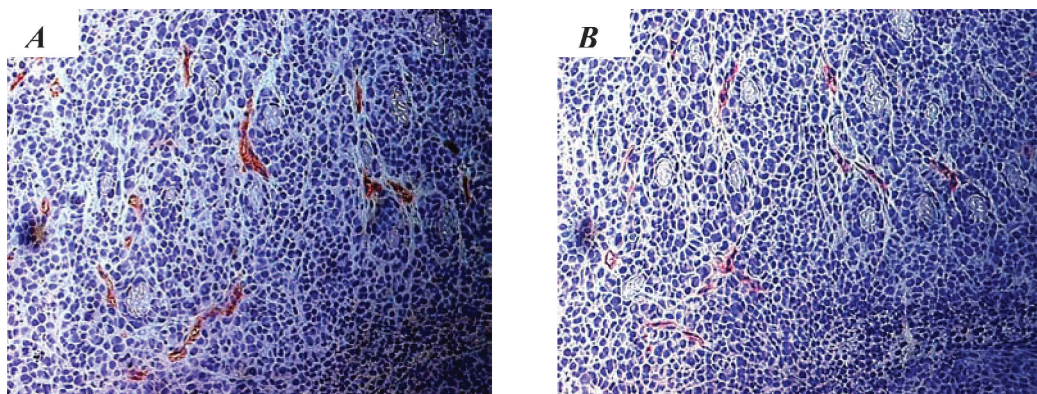


FIG. 4. Typical histological sections of a typical TLT tumor after 2 days of treatment with vandetanib or DMSO. Immunohistological staining was carried out with antibody against CD31. For both groups (panel A: control, panel B: treated), the vessels are evenly distributed throughout the tumor even in the center. No differences in the number of vessels, in dilation or in necrosis were observed between groups.

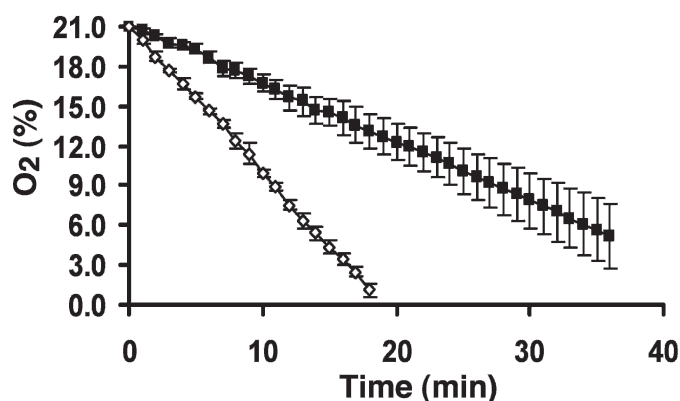


FIG. 5. Effect of *in vivo* vandetanib treatment on rate of oxygen consumption by tumor cells. ■, vandetanib-treated group ($n = 4$); ◇, control group ($n = 3$). Treated tumors consumed oxygen 2.8 times more slowly than control cells. Bars, \pm SE.

vandetanib ($n = 5$) groups, respectively]. In conclusion, no effect of vandetanib on tumor vasculature was apparent after 2 days of treatment.

Effect of Vandetanib on the Rate of Oxygen Consumption by Tumor Cells

The rate of oxygen consumption by TLT tumor cells excised from mice treated with vandetanib for 2 days was significantly reduced ($P < 0.0001$; Fig. 5). The mean slopes were $-1.11 \pm 0.03 \mu\text{M}/\text{min}$ per 2×10^7 cells/ml ($n = 3$) and $-0.44 \pm 0.07 \mu\text{M}/\text{min}$ per 2×10^7 cells/ml ($n = 4$) for the control and vandetanib groups, respectively. This means that cells from vandetanib-treated tumors consumed oxygen 2.8 times more slowly than control cells.

Effect of Vandetanib on Radiation Sensitivity

To assess the therapeutic relevance of the early increase in tumor oxygenation, we combined vandetanib treatment (2 days) with 10 Gy radiotherapy. Figure 6A shows the growth of TLT tumors that were injected with vandetanib or DMSO for 2 days with or without irradiation 24 h after the second injection. Without irradiation, vandetanib treatment did not significantly affect the tumor growth ($P > 0.05$). The time to reach 12 mm in size was 12.2 ± 0.5 days ($n = 6$) and 10.4 ± 1.1 days ($n = 7$) for the treated and control groups, respectively. When the tumors were irradiated with 10 Gy without vandetanib, pretreatment growth was significantly delayed; the time to reach 12 mm was 16.6 ± 1.3 days ($n = 8$). The treatment with vandetanib before irradiation led to a significant increase ($P < 0.01$) in tumor growth delay (24.9 ± 1.5 days to reach 12 mm, $n = 5$). To discriminate between an oxygen effect and a direct radiosensitizing effect, radiosensitivity was tested in TLT cells irradiated in the presence of vandetanib (Fig. 6B). A 2-Gy dose was used because it is the dose that induces about 50% tumor cell death. Compared to control cells, vandetanib did not exert any sensitizing effect. Meanwhile, irradiation with 2 Gy led to a significant

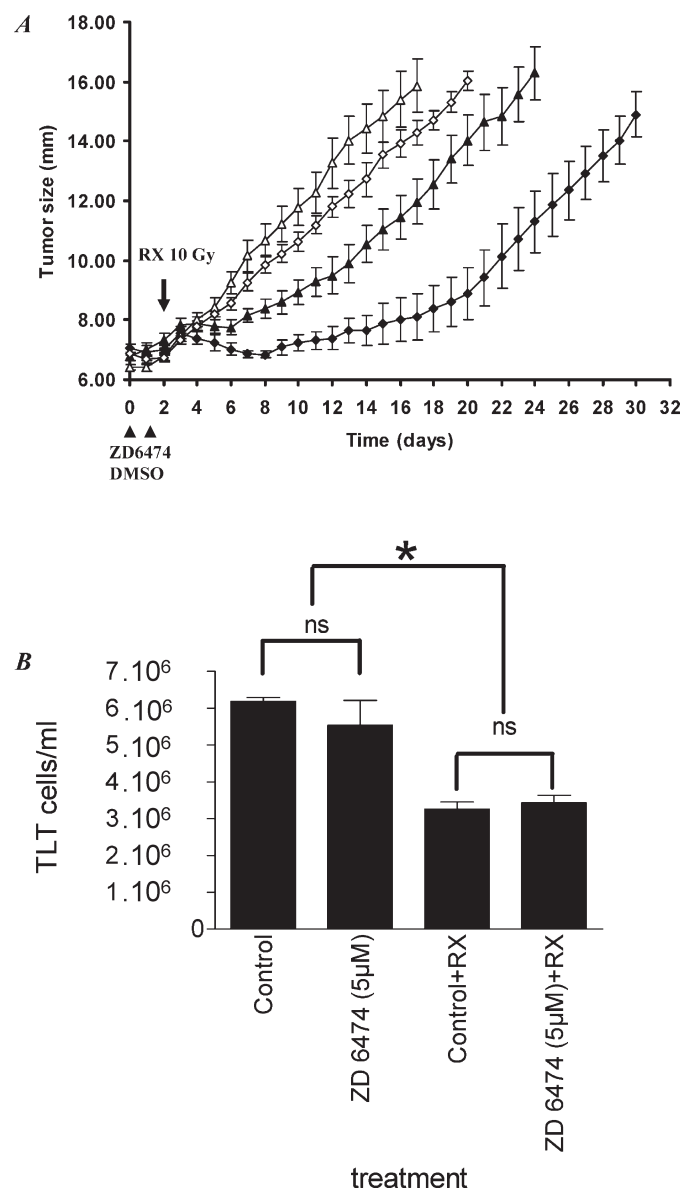


FIG. 6. Panel A: Effect of the combination of vandetanib and radiation (RX) on TLT tumor regrowth. Mice were treated with vandetanib (◇; $n = 6$), with DMSO (△; $n = 7$), with 10 Gy of radiation after 2 days of DMSO (▲; $n = 8$), or with 10 Gy of radiation after 2 days of vandetanib (◆; $n = 5$). Each point represents the mean tumor size \pm SE. No difference in regrowth delay was observed between the control and the vandetanib-treated groups (without radiation). Delays in regrowth to 12 mm in diameter were 16.6 ± 1.3 days for control + radiation and 24.9 ± 1.5 days for vandetanib + radiation ($P < 0.01$). Vandetanib increased the regrowth delay by a factor of 2.3. Panel B: Effect of vandetanib (5 μM) on TLT cells evaluated by the Trypan blue dye exclusion assay. This technique showed that 2 Gy of radiation affected the tumor cells. Nevertheless, vandetanib did not exert any cytotoxic or sensitizing effect. * $P < 0.05$; ns: not significant.

decrease in tumor cell numbers in both experiments ($P < 0.01$). These survival assays using dye exclusion were performed because the classical clonogenic assay was impossible in this model. Overall, these observations suggest that vandetanib radiosensitizes TLT tumors

through changes in tumor oxygenation rather than by a direct sensitizing effect.

DISCUSSION

The major findings of the present study are the following: (a) vandetanib, a selective VEGFR-2 tyrosine kinase inhibitor, induces an increase in tumor oxygenation at an early phase of treatment; (b) this tumor reoxygenation can be exploited to increase the efficacy of combined radiotherapy; (c) the mechanism of increase in tumor oxygenation does not involve a “normalization” of the tumor vasculature as described previously for thalidomide in the same tumor model (3, 4) but is consistent with the decrease in the oxygen consumption by the tumor cells, as described for SU5416 (16).

Few studies have focused on the evolution of the tumor microenvironment during anti-angiogenic therapy, although it has been demonstrated that a transient process called tumor vasculature normalization can occur (2), which may be relevant to treatment outcome using combined therapies (3–12). More recently, we demonstrated that besides this normalization process, a reduction in the consumption of oxygen by tumor cells could also induce an increase in tumor oxygenation after anti-angiogenic treatment (16). We used vandetanib, a promising anti-angiogenic agent under evaluation in Phase III clinical trials in NSCLC (30), to determine whether reoxygenation is a common feature of the early phase of treatment with anti-angiogenic agents. Our results indicate that vandetanib induces an increase in tumor pO_2 during 2 days of treatment (Fig. 2). This transient tumor reoxygenation is comparable to the effect observed after other anti-angiogenic treatments (3, 4, 16) in the same tumor model and could be the result of the ability of vandetanib to modify tumor microenvironment parameters. At this early stage of the treatment, no apparent remodeling of the tumor vasculature (Fig. 3) and no changes in tumor perfusion and permeability parameters (Fig. 2) were observed. Hence vandetanib is clearly distinguishable from thalidomide (3), and a mechanism other than “tumor vasculature normalization” is responsible for this effect. We demonstrated a reduction in tumor oxygen consumption after vandetanib treatment. The reduction factor in oxygen consumption observed is sufficient to abolish tumor hypoxia, as we reported previously using other treatments (29, 31). Overall, the changes observed in the tumor microenvironment in the early phase are similar to those observed using SU5416, another inhibitor of the VEGF-R2 receptor (16).

Why is vandetanib unable to modify the hemodynamics in TLT tumors? One possible explanation is that the TLT tumor is a highly proliferative model in which the inhibitory effects of vandetanib could be suppressed by the rapid turnover of VEGFR-2 (FLK-1) (32). The

TLT tumor model is distinguishable from other tumor models, because it has been shown that vandetanib was able to decrease both flow and permeability in human colon tumors (33) and was able to induce transient normalization of the vasculature in gliomas (9). Another possible explanation is that inhibition of VEGF/VEGFR signaling may be compensated by another angiogenic pathway such as bFGF, platelet-derived growth factor (PDGF), transforming growth factor (TGF)- β , or Tie-2 signaling (34, 35). The fact that thalidomide was able to induce a transient normalization of tumor vasculature in the same tumor model is consistent with this hypothesis, because thalidomide acts on different angiogenic pathways. Whatever the cause of this absence of effect on the tumor hemodynamics, this led us to identify oxygen consumption as a possible target of vandetanib.

These results may have clinical relevance for the combination of vandetanib with radiotherapy. Various preclinical and clinical studies have already been performed and have shown a benefit outcome with combined therapies (19, 36), but no study has focused on the evolution of the tumor microenvironment. Ionizing radiation is known to induce the expression of VEGF, and the inhibition of VEGF activity may inhibit VEGF-induced protection of endothelial cells and enhance tumor cell apoptosis. In addition, the results of the current study suggest that vandetanib can lead to profound alterations in tumor oxygenation in the early phase of treatment that can be exploited when it is combined with radiotherapy. Our study clearly reported that 2 days of vandetanib treatment potentiated the effects of 10 Gy radiotherapy compared to vandetanib alone or radiotherapy alone. It is important to note that this change in sensitivity to radiation is not the result of a direct additive tumor cell toxicity (Fig. 5). Vandetanib alone did not induce a marked growth delay in this fast-growing tumor after 2 days of exposure, strongly suggesting an effect mediated by changes in the tumor microenvironment rather than a direct effect on tumor cells. Because the transient tumor reoxygenation is not correlated with an improvement in tumor perfusion, we can reasonably ascribe this effect to the decrease in tumor cell oxygen consumption.

Other groups found an impact of ZD6474 on clonogenic survival after radiation treatment of glioma cells (36). This confirms that additional preclinical studies on different tumor models are required. The therapeutic relevance in terms of radiation sensitivity also needs to be examined with a tumor control dose assay (TCD₅₀) before clinical use. Finally, the relevance of these mechanisms in human tumors still needs to be elucidated. However, although several mechanisms may contribute to the potentiating effect of vandetanib on radiotherapy, our present study suggests that individual monitoring of the tumor microenvironment is warranted

during the early phase of vandetanib treatment. This may lead to the identification of an optimal therapeutic window for administering vandetanib in combination with radiotherapy.

These data are consistent with previous studies that identified the inhibition of mitochondrial respiration as a particularly interesting target in combined anticancer therapies (16, 29, 31, 37, 38). Optimal dosing and scheduling of novel agents combined with radiotherapy need to be determined and are likely to differ from one tumor type to another. The long-term inhibition of oxygen consumption occurring during treatment with an inhibitor of VEGFR-2 signaling may enhance the outcome of radiotherapy. Our results strongly suggest that the mitochondrial respiratory chain may be a downstream pathway affected by anti-angiogenic therapies targeted against VEGFR-2 (anti Flk-1/KDR) and that the resulting modulation of tumor oxygenation can be exploited to improve the efficacy of combination radiotherapy.

ACKNOWLEDGMENTS

This work was supported in part by grants from the Belgian National Fund for Scientific Research (F.N.R.S) (grant 7.4503.02), the Fonds Joseph Maisin, and the "Actions de Recherches Concertées - Communauté française de Belgique 04/09-317". R.A. is FNRS-Televie fellow. BFJ is FNRS Research Associate. The authors thank AstraZeneca (Macclesfield, UK) for providing vandetanib and Guerbet Laboratories (Roissy, France) for providing P792.

Received: February 10, 2009; accepted: June 5, 2009

REFERENCES

1. J. Folkman, Role of angiogenesis in tumor growth and metastasis. *Semin. Oncol.* **29**, 15–18 (2002).
2. R. K. Jain, Normalization of tumor vasculature: an emerging concept in antiangiogenic therapy. *Science* **307**, 58–62 (2005).
3. R. Ansiaux, C. Baudelet, B. F. Jordan, N. Beghein, P. Sonveaux, J. Dewever, P. Martinive, V. Grégoire, O. Feron and B. Gallez, Thalidomide radiosensitizes tumors through early changes in the tumor microenvironment. *Clin. Cancer Res.* **11**, 743–750 (2005).
4. J. Segers, V. D. Fazio, R. Ansiaux, P. Martinive, O. Feron, P. Wallemacq and B. Gallez, Potentiation of cyclophosphamide chemotherapy using the anti-angiogenic drug thalidomide: Importance of optimal scheduling to exploit the 'normalization' window of the tumor vasculature. *Cancer Lett.* **244**, 129–135 (2006).
5. S. Vosseler, N. Mirancea, P. Bohlen, M. M. Mueller and N. E. Fusenig, Angiogenesis inhibition by vascular endothelial growth factor receptor-2 blockade reduces stromal matrix metalloproteinase expression, normalizes stromal tissue, and reverts epithelial tumor phenotype in surface heterotransplants. *Cancer Res.* **65**, 1294–1305 (2005).
6. F. Winkler, S. V. Kozin, R. T. Tong, S. S. Chae, M. F. Booth, I. Garkavtsev, L. Xu, D. J. Hicklin and R. K. Jain, Kinetics of vascular normalization by VEGFR2 blockade governs brain tumor response to radiation: role of oxygenation, angiopoietin-1, and matrix metalloproteinases. *Cancer Cell.* **6**, 553–563 (2004).
7. R. T. Tong, Y. Boucher, S. V. Kozin, F. Winkler, D. J. Hicklin and R. K. Jain, Vascular normalization by vascular endothelial growth factor receptor 2 blockade induces a pressure gradient across the vasculature and improves drug penetration in tumors. *Cancer Res.* **64**, 3731–3736 (2004).
8. D. Fukumura and R. K. Jain, Tumor microvasculature and microenvironment: targets for anti-angiogenesis and normalization. *Microvasc. Res.* **74**, 72–84 (2007).
9. A. Claes, P. Wesseling, J. Jeuken, C. Maass, A. Heerschap and W. P. Leenders, Antiangiogenic compounds interfere with chemotherapy of brain tumors due to vessel normalization. *Mol. Cancer Ther.* **7**, 71–78 (2008).
10. M. E. Eichhorn, S. Strieth, S. Luedemann, A. Kleespies, U. Nöth, A. Passon, G. Brix, K. W. Jauch, C. J. Bruns and M. Dellian, Contrast enhanced MRI and intravital fluorescence microscopy indicate improved tumor microcirculation in highly vascularized melanomas upon short-term anti-VEGFR treatment. *Cancer Biol. Ther.* **7**, 1006–1013 (2008).
11. Q. Zhou, P. Guo and J. M. Gallo, Impact of angiogenesis inhibition by sunitinib on tumor distribution of temozolomide. *Clin. Cancer Res.* **14**, 1540–1549 (2008).
12. J. Hamzah, M. Jugold, F. Kiessling, P. Rigby, M. Manzur, H. H. Marti, T. Rabie, S. Kaden, H. J. Gröne and R. Ganss, Vascular normalization in Rgs5-deficient tumours promotes immune destruction. *Nature* **453**, 410–414 (2008).
13. R. K. Jain, D. G. Duda, J. W. Clark and J. S. Loeffler, Lessons from phase III clinical trials on anti-VEGF therapy for cancer. *Nat. Clin. Pract. Oncol.* **3**, 24–40 (2006).
14. C. G. Willett, Y. Boucher, D. G. Duda, E. di Tomaso, L. L. Munn, R. T. Tong, S. V. Kozin, L. Petit, R. K. Jain and G. Y. Lauwers, Surrogate markers for antiangiogenic therapy and dose-limiting toxicities for bevacizumab with radiation and chemotherapy: continued experience of a phase I trial in rectal cancer patients. *J. Clin. Oncol.* **23**, 8136–8139 (2005).
15. R. K. Jain, Normalizing tumor vasculature with anti-angiogenic therapy: a new paradigm for combination therapy. *Nat. Med.* **7**, 987–989 (2001).
16. R. Ansiaux, C. Baudelet, B. F. Jordan, N. Crockart, P. Martinive, J. DeWever, V. Grégoire, O. Feron and B. Gallez, Mechanism of reoxygenation after antiangiogenic therapy using SU5416 and its importance for guiding combined antitumor therapy. *Cancer Res.* **66**, 9698–9704 (2006).
17. S. R. Wedge, D. J. Ogilvie, M. Dukes, J. Kendrew, R. Chester, J. A. Jackson, S. J. Boffey, P. J. Valentine, J. O. Curwen and L. F. Hennequin, ZD6474 inhibits vascular endothelial growth factor signaling, angiogenesis, and tumor growth following oral administration. *Cancer Res.* **62**, 4645–4655 (2002).
18. A. J. Ryan and S. R. Wedge, ZD6474—a novel inhibitor of VEGFR and EGFR tyrosine kinase activity. *Br. J. Cancer* **92**(Suppl.), S6–S13 (2005).
19. B. Frederick, D. Gustafson, C. Bianco, F. Ciardiello, I. Dimery and D. Raben, ZD6474, an inhibitor of VEGFR and EGFR tyrosine kinase activity in combination with radiotherapy. *Int. J. Radiat. Oncol. Biol. Phys.* **64**, 33–37 (2006).
20. F. Ciardiello, R. Caputo, V. Damiano, T. Troiani, D. Vitagliano, F. Carlomagno, B. M. Veneziani, G. Fontanini, A. R. Bianco and G. Tortora, Antitumor effects of ZD6474, a small molecule vascular endothelial growth factor receptor tyrosine kinase inhibitor, with additional activity against epidermal growth factor receptor tyrosine kinase. *Clin. Cancer Res.* **9**, 1546–1556 (2003).
21. M. F. McCarty, J. Wey, O. Stoeltzing, W. Liu, F. Fan, C. Bucana, P. F. Mansfield, A. J. Ryan and L. M. Ellis, ZD6474, a vascular endothelial growth factor receptor tyrosine kinase inhibitor with additional activity against epidermal growth factor receptor tyrosine kinase, inhibits orthotopic growth and angiogenesis of gastric cancer. *Mol. Cancer Ther.* **3**, 1041–1048 (2004).
22. J. N. Rich, S. Sathornsumetee, S. T. Keir, M. W. Kieran, A. Laforme, A. Kaipainen, R. E. McLendon, M. W. Graner, B. K. Rasheed and H. S. Friedman, ZD6474, a novel tyrosine kinase inhibitor of vascular endothelial growth factor receptor and epidermal growth factor receptor, inhibits tumor growth of multiple nervous system tumors. *Clin. Cancer Res.* **11**, 8145–8157 (2005).

23. S. Rehman and G. C. Jayson, Molecular imaging of antiangiogenic agents. *Oncologist* **10**, 92–103 (2005).
24. B. Gallez, B. F. Jordan, C. Baudelet and P. D. Misson, Pharmacological modifications of the partial pressure of oxygen in tumors. Evaluation using *in vivo* EPR oximetry. *Magn. Reson. Med.* **42**, 627–630 (1999).
25. B. Gallez, C. Baudelet and B. F. Jordan, Assessment of tumor oxygenation by electron paramagnetic resonance: principles and applications. *NMR Biomed.* **17**, 240–262 (2004).
26. H. S. Taper, G. W. Woolley, M. N. Teller and M. P. Lardis, A new transplantable mouse liver tumor of spontaneous origin. *Cancer Res.* **26**, 143–148 (1966).
27. C. Baudelet, R. Ansiaux, B. F. Jordan, X. Havaux, B. Macq AND B. Gallez, Physiological noise in murine solid tumor using T2*-weighted gradient-echo imaging: a marker of tumour acute hypoxia? *Phys. Med. Biol.* **49**, 3389–3411 (2004).
28. S. M. Galbraith, R. J. Maxwell, M. A. Lodge, G. M. Tozer, J. Wilson, N. J. Taylor, J. J. Stirling, L. Sena, A. R. Padhani and G. J. Rustin, Combrestatin A4 phosphate has tumor antivascular activity in rat and man as demonstrated by dynamic magnetic resonance imaging. *J. Clin. Oncol.* **21**, 2831–2842 (2003).
29. B. F. Jordan, V. Grégoire, R. J. Demeure, P. Sonveaux, O. Feron, J. O'Hara, V. P. Vanhulle, N. Delzenne and B. Gallez, Insulin increases the sensitivity of tumors to irradiation: involvement of an increase in tumor oxygenation mediated by a nitric oxide-dependent decrease of the tumor cells oxygen consumption. *Cancer Res.* **62**, 3555–3561 (2002).
30. A. Morabito, E. De Maio, M. Di Maio, N. Normanno and F. Perrone, Tyrosine kinase inhibitors of vascular endothelial growth factor receptors in clinical trials: current status and future directions. *Oncologist* **11**, 753–764 (2006).
31. N. Crockart, K. Radermacher, B. F. Jordan, C. Baudelet, G. O. Cron, V. Grégoire, N. Beghein, C. Bouzin, O. Feron and B. Gallez, Tumor radiosensitization by antiinflammatory drugs: evidence for a new mechanism involving the oxygen effect. *Cancer Res.* **65**, 7911–7916 (2005).
32. T. Takamoto, M. Sasaki, T. Kuno and N. Tamaki, Flk-1 specific kinase inhibitor (SU5416) inhibited the growth of GS-9L glioma in rat brain and prolonged the survival. *Kobe J. Med. Sci.* **47**, 181–191 (2001).
33. D. P. Bradley, J. L. Tessier, D. Checkley and H. Kuribayashi, Effects of AZD2171 and vandetanib (ZD6474, Zactima) on haemodynamic variables in an SW620 human colon tumour model: an investigation using dynamic contrast-enhanced MRI and the rapid clearance blood pool contrast agent, P792 (gadomelitol). *NMR Biomed.* **21**, 42–52 (2008).
34. J. Folkman, T. Browder and J. Palmblad, Angiogenesis research: guidelines for translation to clinical application. *Thromb. Haemost.* **86**, 23–33 (2001).
35. A. Stratmann, W. Risau and K. H. Plate, Cell type-specific expression of angiopoietin-1 and angiopoietin-2 suggests a role in glioblastoma angiogenesis. *Am. J. Pathol.* **153**, 1459–1466 (1998).
36. V. Damiano, D. Melisi, C. Bianco, D. Raben, R. Caputo, G. Fontanini, R. Bianco, A. Ryan, A. R. Bianco and G. Tortora, Cooperative antitumor effect of multitargeted kinase inhibitor ZD6474 and ionizing radiation in glioblastoma. *Clin. Cancer Res.* **11**, 5639–5644 (2005).
37. J. E. Biaglow, Y. Manevich, D. Leeper, B. Chance, M. W. Dewhirst, W. T. Jenkins, S. W. Tuttle, K. Wroblewski, J. D. Glickson and S. M. Evans, MIBG inhibits respiration: potential for radio- and hyperthermic sensitization. *Int. J. Radiat. Oncol. Biol. Phys.* **42**, 871–876 (1998).
38. T. W. Secomb, R. Hsu, E. T. Ong, J. F. Gross and M. W. Dewhirst, Analysis of the effects of oxygen supply and demand on hypoxic fraction in tumors. *Acta Oncol.* **34**, 313–316 (1995).